RESTRUCTURING BATCH NORMALIZATION TO ACCELERATE CNN TRAINING

Anonymous Authors[1]

ABSTRACT

In this paper, we focus on the acceleration of the batch normalization (BN) layers among the non-convolutional layers within Convolutional Neural Network (CNN) models, as BN has become a core design block of modern CNNs with smaller convolutional (CONV) filters. A typical modern CNN has a large number of BN layers in its lean and deep architecture. BN requires mean and variance calculations over each mini-batch during training. Therefore, the existing memory access reduction techniques, such as fusing multiple CONV layers, are not effective for accelerating BN due to their inability to optimize mini-batch related calculations. To address this increasingly important problem, we propose to restructure BN layers by first splitting a BN layer into two sub-layers (fission) and then combining the first sub-layer with its preceding CONV layer and the second sub-layer with the following activation and CONV layers (fusion). The proposed solution can significantly reduce main-memory accesses while training the latest CNN models, and the experiments on a chip multiprocessor show that the proposed BN restructuring can improve the performance of DenseNet-121 by 25.7%.

1 INTRODUCTION

Deep Neural Networks (DNNs) have emerged as the key technique of artificial intelligence, and Convolutional Neural Networks (CNNs) (He et al., 2016b; Huang et al., 2017; Krizhevsky et al., 2012) are widely used for image classification and object detection tasks. Typical DNNs, which consist of multiple stacked layers and multiple channels (filters) per layer, require billions of operations (Canziani et al., 2016) for training and inference, and CNNs usually require larger amount of operations than other types of DNNs. As the first order of solution to the computational load problem, hardware accelerators such as GPGPUs (Foley & Danskin, 2017), FPGAs (Alwani et al., 2016), ASICs (Jouppi et al., 2017), and manycore processors (Sodani et al., 2016) have been developed. Then, further optimization was performed for CNNs. For the CNNs designed in the early days, convolutional (CONV) and fully-connected (FC) layers were the most time-consuming parts, and the CNN accelerator research has mainly focused on optimizing the two layer types. For example, loop blocking and reordering techniques were highly effective for maximizing data reuse of CONV/FC layers (Yang et al., 2016; Chen et al., 2016b), and subsequently network compression or approximate computing methods were shown to significantly reduce computation and memory access (Han et al., 2016a;b; 2015; Sriniva & Babu, 2015). Previous works, however, paid almost no attention to the *non-CONV* layers as their influence on resource consumption was ignorable.[1]

The latest CNN models such as ResNet (He et al., 2016b) and DenseNet (Huang et al., 2017), however, are actively adopting new structures and non-CONV layers to improve prediction performance. For instance, *skip connection* has been utilized to stabilize backpropagation and to enable stacking of hundreds of layers; and Batch Normalization (BN) was developed to address *internal covariate shift* phenomenon (Ioffe & Szegedy, 2015). With the invention of many new layer types which enables more layers to be stacked, the relative portion of non-CONV layers in a CNN model has been increasing. On the contrary, the computation load of CONV layers has been declining because of the reductions in the size of the convolution filters. The early CNN models such as AlexNet (Krizhevsky et al., 2012) and VGG (Simonyan & Zisserman, 2014) have used convolution filters with the size of 3×3, 5×5, 7×7, and even 11×11. But the recent designs such as ResNet and DenseNet apply 1×1 or 3×3 filters in many parts of CONV layers and successfully reduce the computational overhead. Overall, all the design trends of modern CNNs indicate that the importance of CONV/FC layers is decreasing while the importance of non-CONV layers is increasing.

While we expect many non-CONV layers to be developed and become a significant part of computational load, as of today, BN during the training phase is known as the most computationally intensive non-CONV layer. Training is the process of using the labeled data to decide the network parameter values, and inference is the process of using the trained network to generate classification or other output

[1] We address layers other than CONV/FC as non-CONV layers.

results for previously unseen input data. One might think inference is much more important because training needs to be completed only once; but in reality, training needs to be performed repeatedly by trying different hyperparameters such as network depth, number of neurons, learning rate, regularizer, optimizer, and activation function (Bergstra & Bengio, 2012; Snoek et al., 2012). Even after a training is deemed to be complete and the trained network is deployed for a real service, deep learning research is moving so fast that the developers are immediately forced to consider newly invented solutions to replace the deployed one. Therefore, both researchers and practitioners end up spending a significant portion of their computational resources on training, and improving the performance of training process is as important as (or arguably even more important than) improving that of inference process.

During training, a BN layer requires per-channel mean and variance of input elements to be evaluated over the entire mini-batch dataset. There are other layers and operations that require statistics to be calculated over the entire mini-batch dataset (e.g., covariance matrix for regularization (Cogswell et al., 2016) and mutual information for disentangling GAN representations (Chen et al., 2016a)), but BN has the largest impact on computational load as it is currently very popular and it can be included in multiple places within a deep learning network. As in (Alwani et al., 2016) where intermediate data between layers was recognized as an opportunity to accelerate CNN inference, we recognize that the mini-batch calculation of BN is an opportunity as well. However, as opposed to (Alwani et al., 2016), we focus on restructuring BN because BN during training imposes strict dependency across a large volume of mini-batch dataset which does not fit within on-chip buffers and hence fusing multiple convolutional layers is less attractive.

In this paper, we develop a BN restructuring solution for the latest CNN models making the following key contributions:

- We explore the execution time breakdowns and show that non-CONV layers have become significantly more important for the latest CNN models. We also show that BN is the most important among non-CONV layer types.
- We propose a novel BN layer restructuring where a BN layer is first divided into sub-layers (fission) and then merged with neighboring layers (fusion). This restructuring can significantly mitigate memory bottleneck problem by reducing memory traffic concentrated on BN layers.
- We achieve 25.7% of performance enhancement on the latest commercial chip multiprocessor (Intel's Skylake (Doweck et al., 2017)) on top of a highly-optimized CNN library (Intel, 2016). Applying the BN restructuring to GPU with an open-source linear algebra library (Kerr et al., 2017) also improves performance by 17.4%.

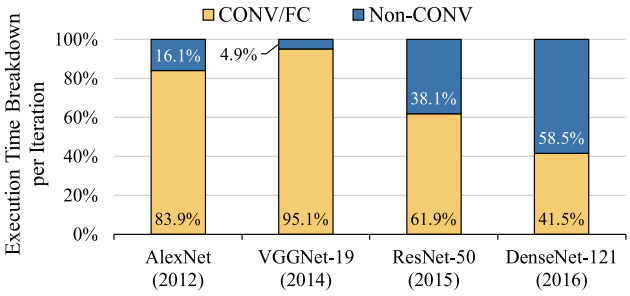

Figure 1. Execution time breakdown of popular CNN models over layer types. We categorize CONV and FC layers into a group and the remaining layers into the other (non-CONV). On early CNN models, CONV/FC layers dominate execution time, whereas more recent/deeper CNN models consume a significant portion of execution time for non-CONV layers.

2 Background and Motivation

2.1 Trends in CNN accelerator designs

Many CNN accelerator proposals and designs are mainly focused on convolutional (CONV) and fully-connected (FC) layers. This is because those layers take up most of the inference and training time of relatively shallow CNNs (up to few dozens of layers). For example, AlexNet (Krizhevsky et al., 2012) consists of only 5 CONV layers and 3 FC layers, whereas VGGNet (Simonyan & Zisserman, 2014) has 13-16 CONV layers and 3 FC layers. On these early and shallow CNN models, the portion of execution time on CONV and FC layers is dominant, accounting for up to 95% of total execution time as shown in Figure 1 (we measured the training time from the system specified in Section 4).

Common optimization strategies implemented in the CNN accelerators for the two types of layers include: reducing memory bandwidth by maximizing the data reuse of weights, input feature maps, and output feature maps (Chen et al., 2014a; 2016b; Du et al., 2015), pruning redundant parameters (e.g., weights) and exploiting sparsity (Albericio et al., 2016; Han et al., 2016a; Zhang et al., 2016), computing in an approximate manner (Han et al., 2016b; 2015), and adopting new memory technologies (Chi et al., 2016; Kim et al., 2016; Shafiee et al., 2016). However, there are relatively few studies focusing on optimizing the layers other than CONV and FC layers (non-CONV), such as ReLU[2], pooling, and batch normalization (BN) layers because *these non-CONV layers take much less time compared to the CONV and FC layers on these shallow CNNs.*

Recent deeper CNN models (e.g., ResNet (He et al., 2016b) and DenseNet (Huang et al., 2017)) spend a more portion of execution time executing non-CONV layers as opposed

[2]Rectified Linear Unit, replacing negative values into zeros and passes positive values, is mainly used recently for activation.

to the conventional CNN models with shallow layers. For example, DenseNet-121 (DenseNet with 120 CONV layers plus one FC layer) spends more than half of the execution time on the non-CONV layers (see Figure 1). For these CNN models, accelerating the non-CONV layers is gaining more importance.

Optimizing the non-CONV layers is more complicated when it comes to the training process than the inference process. Previous techniques to boost the inference process, such as approximate computing and compression, are not easily applied to the training process because weights are updated in the course of training. Complex data dependency in the training process also matters; a layer performing element-wise operations during inference (e.g., batch normalization (BN), which will be explained further in Section 2.2) demands data from multiple intermediate output values of its previous layers, making optimization a non-trivial task.

The training process matters in that it requires significant computing costs. ResNet-50 takes 29 hours to train with 8 Tesla P100 GPUs, as each epoch (training an entire dataset) consumes 16 minutes for the images of the the ImageNet Large Scale Visual Recognition Challenge dataset (Goyal et al., 2017). Google AlphaGo (Silver et al., 2016) was trained for more than three weeks with 50 GPUs to beat a top-class professional Go player. If training is an one-time event, its cost would be well amortized. However, DNN models evolve rapidly and more data are accumulated, demanding continuous training. These all support the importance of optimizing the CNN training process.

However, relatively few studies have focused on the training process, especially the non-CONV layers. Although several DNN acceleration strategies have been studied to mitigate the computing cost of the training process (Goyal et al., 2017; Rhu et al., 2016; Venkataramani et al., 2017), these are different from our work in that they did not focus on accelerating the non-CONV layers. In this paper, we identify key performance bottlenecks in training non-CONV layers of the latest deeper CNN models and demonstrate performance gain by reducing the number of memory access.

2.2 Trends in recent CNN models

In pursuit of improving the accuracy of CNN models with larger and deeper network, vanishing gradient is one of critical challenges; the vanishing gradient is a phenomenon that errors (gradients) fade out while traversing the backpropagation pass, which prevents the network from converging fast. To overcome this problem, Recent CNN models (e.g., ResNet and DenseNet) have adopted batch normalization (BN) and residual learning (He et al., 2016b).

BN (Ioffe & Szegedy, 2015) was proposed in 2015 for stable learning, which helps solving the vanishing/exploding gradient problem. It normalizes input within a mini-batch (a collection of several inputs among an entire input set) to make the input feature maps follow a Gaussian distribution. Specifically, BN first computes the mean and the variance values for each channel of its input feature maps sweeping through the values over a mini-batch; then it performs normalization, followed by scaling with a scale factor (γ) and by finally adding a shift factor (β). Dropout (Srivastava et al., 2014) also regularizes the network by randomly dropping weights whose rates are also trainable factors, which brings a similar effect compared to BN. In this paper, we target recent and popular CNN models that use BN.

Residual learning is another solution to cope with the degradation problem, which is the phenomenon that increasing network depth does not lead to a better accuracy. Residual learning uses *skip connection*; that is, a layer can skip some layers and connect directly to a layer that is farther away. ResNet, one of the state-of-the-art CNNs (He et al., 2016b), adopted residual learning with identity mapping, which adds a layer to the far layer in an element-wise manner (through an element-wise sum (EWS) layer). This effectively shortens the distance between close-to-input layers and close-to-output layers, enabling very deep networks with hundreds of layers to converge, achieving higher accuracy compared to more shallow models. Due to its record-breaking performance in image recognition, residual learning has frequently been adopted in the latest CNNs (He et al., 2016b;a; Xie et al., 2016). DenseNet (Huang et al., 2017), which we mainly target for optimization, also holds a variant of the residual learning (as what DenseNet refers to *dense connectivity*), which is similar to residual learning in ResNet but in a slightly different way – it concatenates multiple feature maps rather than performs the element-wise sum.

Many non-CONV layer types, such as BN, concatenation (Concat), EWS, and Split, are used in CNN models to properly support the techniques explained above. A Split layer, for example, copies the output feature maps of its preceding layer to multiple following layers; then one of those following layers either concatenates the copied feature maps with its other input feature maps (which is performed at a Concat layer in DenseNet) or performs element-wise summation among the input feature maps from its multiple preceding layers (at EWS layer in ResNet).

The importance of optimizing these non-CONV layers grows as they take a more portion of training time compared to CONV layers. Because smaller CONV filters are more frequently used on modern deeper CNNs, the amount of computation per CONV filter has been decreased. For example, AlexNet includes 11×11 and 5×5 filters, whereas more recent models, such as DenseNet, ResNet, and Inception network (Szegedy et al., 2016), adopt relatively small filters, mainly 3×3 and 1×1.

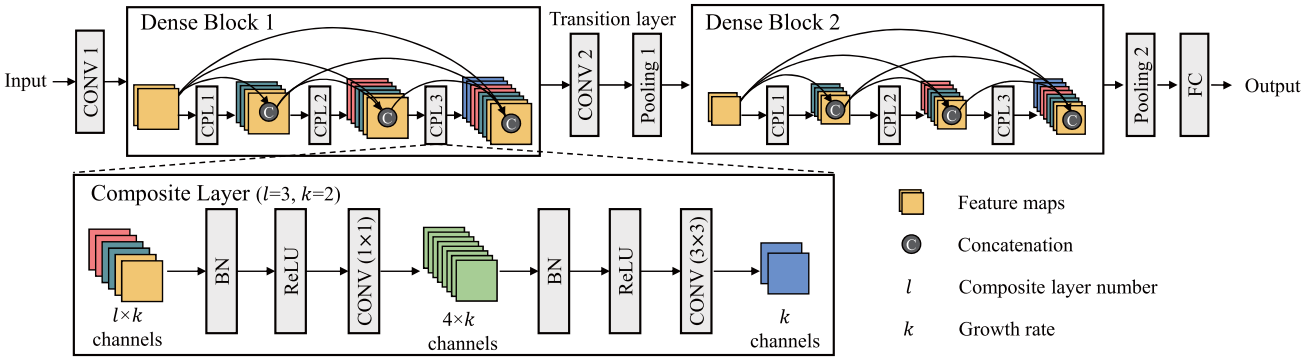

Figure 2. An exemplar DensetNet structure with two Dense Blocks, connected through a transition layer which changes the number and size of the input feature maps to a Dense Block. Each Dense Block has multiple Composite Layers (CPLs), each of which is connected to every other CPL within a Dense Block in a feed-forward fashion. A CPL consists of six layers (BN, ReLU, 1×1 CONV, BN, ReLU, and 3×3 CONV). The 1×1 CONV layer in a CPL, called bottleneck layer, limits the number of input feature maps to 4×k while the second CONV outputs k channels that are concatenated to the input feature maps. Growth rate (k) is the variable for how many feature maps are concatenated per CPL; feature maps stack up as they go through CPLs.

2.3 DenseNet: a state-of-the-art CNN model

DenseNet (Huang et al., 2017) is an example of more recent CNN models that use both BN and residual learning to achieve high accuracy with deeper (possibly surpassing 100) layers and smaller CONV filters. It achieves classification accuracy comparable to ResNet, but with fewer learning parameters. A key feature of DenseNet lies in its dense connectivity. A DenseNet is a sequence of *Dense Blocks* (see Figure 2); two adjacent Dense Blocks are connected through transition layers (e.g., few CONV and pooling layers). Each Dense Block has multiple *Composite Layers* (CPLs). A CPL consists of a sequence of BN, ReLU, 1×1 CONV, BN, ReLU, and 3×3 CONV layers. The lth CPL within a Dense Block receives l×k input feature maps (channels). The first 1×1 CONV layer limits the number of feature maps to m×k; when l > m, the 1×1 CONV layer effectively reduces the computation cost of its following sequence of BN, ReLU, and 3 × 3 CONV layers, and hence called a bottleneck layer. All CPLs within a Dense Block is fully connected utilizing Concat and Split layers in a feed-forward fashion (connections not forming a cycle). Feature map size grows within a Dense Block; because the output feature maps from the preceding CPLs are concatenated, a CPL located later (farther from input) in a Dense Block has more input feature maps (channel). A transition layer works similar to a bottleneck layer, limiting the number of channels.

Dense connectivity enables DenseNet to reduce computation cost from CONV layers. It embodies residual learning exploiting skip connection; however, as opposed to ResNet which performs EWS, DenseNet concatenates feature maps from preceding layers. CPL exploits the observation from empirical data that placing the BN layer before ReLU and CONV layers provides better recognition performance (Huang et al., 2017). Furthermore, DenseNet has shown that relatively small k is sufficient in achieving a state-of-the-art accuracy on recognition, as information in feature maps is transferred through dense connectivity. The result is higher computation efficiency in these CONV layers. While non-CONV layers such as BN, ReLU, and Split have been gaining prominence not only in DenseNet but also in other modern CNNs (He et al., 2016b; Howard et al., 2017; Szegedy et al., 2016), an improved degree of computation efficiency in CONV layers due to the aforementioned reasons makes optimizations for non-CONV layers even more important. Therefore, we examine the characteristics of computational challenges in DenseNet and propose solutions to overcome these.

3 BN Restructuring

3.1 Analyzing DenseNet

In this paper, we focus on analyzing the memory access characteristics of CNN layers over time in training DenseNet-121, one of the latest CNN models. For the analysis, we use the latest chip multiprocessor (Intel Skylake (Doweck et al., 2017)) which can be used to measure various architectural statistics (e.g., memory accesses and cache misses) and also provide decent memory bandwidth and computing power. Our observations can also be leveraged to optimize other CNN acceleration platforms and latest CNN models with BN and residual learning, such as ResNet.

We observed the following key memory access characteristics in training DenseNet. First, similar to other CNN models, DenseNet exhibits repeating patterns in memory traffic because layers are processed sequentially and a set of layers with different computational characteristics are executed repeatedly. Second, memory bandwidth demands are different from layer to layer even if both are the same

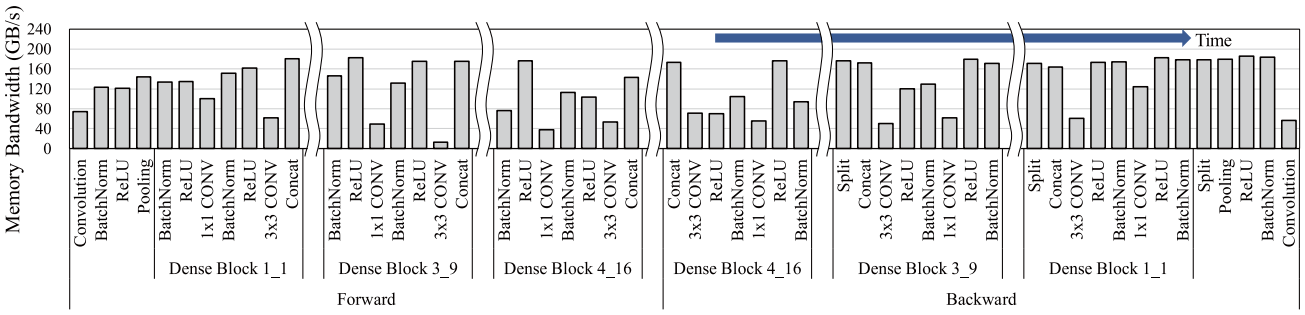

Figure 3. Memory bandwidth utilization of layers on the DenseNet-121 CNN model over time (Huang et al., 2017). Each CONV layer is interleaved with other operation types, such as BN, ReLU, and Concat (concatenation), each exhibiting different degrees of bandwidth demand. Peak main-memory bandwidth of the evaluated system is 230.4GB/s (12 DDR4-2400 channels).

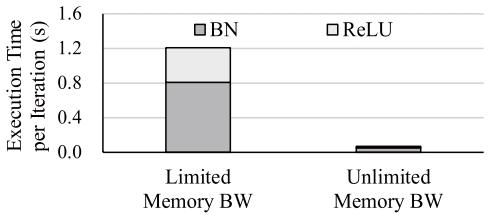

Figure 4. Comparing execution time of BN and ReLU layers with finite and infinite (hypothetical) memory bandwidth.

layer type. This is because each has a different number of input feature maps (ifmaps), output feature maps (ofmaps), and filter sizes to enhance recognition performance and to make operations more efficient. For example, CONV layers with smaller filter sizes have relatively higher memory access rates compared to the total amount of computation because the reuse rate of ifmaps within on-chip buffers is low, whereas layers that use relatively large filter sizes can reduce the off-chip memory bandwidth due to the higher reuse rate of ifmaps. Actually, DenseNet has higher memory bandwidth demands compared to early CNN models as it uses 1×1 CONV and 3×3 CONV layers except the first 7×7 CONV layer (see Figure 3).

Memory bandwidth demand varies greatly between CONV layers and non-CONV layers due to difference in computational characteristics. The non-CONV layers of DenseNet-121 are mostly bottlenecked by the peak main-memory bandwidth of the system we use (230.4GB/s, more details being specified in Section 4), whereas the CONV layers underutilize the available bandwidth (only up to 120GB/s). This is because the non-CONV layers have less data locality and computation intensity, which makes loop blocking techniques less effective, leading to higher demand in memory bandwidth.

If a system has infinite memory bandwidth, the high memory bandwidth demand of the non-CONV layers would not be a problem as the execution time of them would be limited by computation power (peak FLOPS) of the system and the non-CONV layers are much less computationally intensive compared to the CONV layers. However, improving the performance (i.e., bandwidth and latency) of the main-memory systems has remained relatively challenging, as opposed to the rapid growth in computational power (i.e., FLOPS or OPS) per device. Modern data-parallel architectures used for CNN acceleration still provide around hundreds of GB/s of main-memory bandwidth (e.g., 732GB/s with Nvidia Tesla P100 (Foley & Danskin, 2017)) due to the power and signal integrity issues; even if the absolute data transfer rate is impressive, it is not high enough to completely satisfy the bandwidth demands from memory intensive (computationally less intensive) layers, especially BN and ReLU. The maximum computing power of Tesla P100 is 10.6TFLOPS (single-precision floating point), being translated to 14.5FLOP/B or 58 FLOPs per 32-bit data. Assuming that ReLU requires one clipping operation per 32-bit data, 58× more main-memory bandwidth is needed to match P100's computing power.

We tested the portion of BN and ReLU layers from the real machine (Intel Skylake) with a hypothetical model with infinite memory bandwidth for the BN and ReLU layers (Figure 4). To simulate the hypothetical machine, we made BN and ReLU layers skip DRAM memory access by manipulating memory address offsets, thereby all data accesses can fit in L1 caches but the number of operations being executed remains unchanged. In this experiment, we exclude Concat and Split layers because such layers mainly perform memory copies that can be optimized by passing pointers instead of physical copies even if they demand high memory bandwidth in our reference implementation (Yang, 2017) using MKL-DNN (Intel, 2016). We observe that without the bandwidth limitation, the BN and ReLU layers enjoy 20× speedup. If computational power (peak FLOPS) is improved faster than main-memory bandwidth (peak GB/s) in future CNN accelerators, which is quite likely as compu-

tation is cheap and communication is expensive (Han et al., 2016a) in contemporary VLSI systems, the portion of these non-CONV layers in total execution time could even be larger in future. Therefore, it is important to reduce memory accesses on those layers.

Most of memory accesses in ReLU and BN layers come from reading and writing ifmaps and ofmaps. The aggregate size of these feature maps across a mini-batch at a given layer could be too large to fit in on-chip memory with MBs of capacity especially when the size of a mini-batch reaches or surpasses 100, which is preferred as larger mini-batch sizes typically lead to better accuracy. To decrease the memory accesses in these layers, we can consider maximizing data reuse of the ifmaps and the ofmaps between and within the layers. However, because BN layers have strict data dependency, cross-layer data reuse is prohibited. In the forward pass of a BN layer, all pixels of ifmaps that belong to a mini-batch should be retrieved to get per-channel mean and variance values prior to normalizing individual pixels. Likewise, in backpropagation, calculating the partial derivatives on γ (scaling factors) and β (shift factors) accompanies sweeping the partial derivatives on ofmaps; this should precede computing the partial derivatives on ifmaps. Because these dependencies make data reuse distance far in BN, it is difficult to apply the data reuse techniques that were previously proposed for CONV layers to these non-CONV layers. A prior work (Alwani et al., 2016) that tries to fuse multiple CONV layers utilizes data reuse between CONV layers; however, because BN layers are frequently inserted between CONV layers (e.g., each CONV layer within a CPL of DenseNet (Figure 2) is paired with a BN layer) and BN imposes strict dependency, inter-CONV fusion is not attractive to the latest deeper CNNs. With this motivation, we suggest *Fission-n-Fusion*, a novel solution that copes with this strict data dependency in BN layers to minimize unnecessary data transfers.

3.2 Fission-n-Fusion

We first divide the BN layers within the CPLs of DenseNet into two sub-layers (Fission). Then, we combine the first sub-layer with its preceding CONV layer and the second sub-layer with both the ReLU layer and the following CONV layer (Fusion). Fusing multiple (sub-)layers can significantly reduce off-chip memory accesses of BN layers. Fission aids Fusion to be more effective by enabling the operations of a BN layer with the strict data dependency to be entirely fused to its preceding layer and following CONV layer, through which all memory accesses from the original BN layers can be removed. The resulting combination of the two ideas, BN Fission-n-Fusion (BNFF), can save a significant amount of memory access per training step, which is translated to substantial performance improvement.

Figure 5 illustrates how our proposed BNFF is applied to the reference DenseNet implementation (Yang, 2017) that is represented using computational graphs. A grey box is a computational node that accompanies sweeping (reading or writing) all ifmaps or ofmaps of a channel within a mini-batch; this sweeping cannot be filtered by on-chip buffers because the aggregate size of an ifmap and ofmap across a mini-batch of 100 or more images is too large to fit in on-chip buffers, as explained in Section 3.1. An arrow indicates data flow between the computational node, composing dependency. A dotted box represents a layer before and after BNFF. We also present multiple memory accesses to the same feature map with the shapes of the same color (e.g., O_1, I_2, I_3, and I_4 in the forward pass).

During training, a BN layer of the reference implementation accesses the same ifmap and the derivatives on the ofmap multiple times due to data dependency on both forward and backward passes. On the forward pass, a BN layer reads ifmaps three times (I_2, I_3, I_4 in the upper half of Figure 5(a)) and writes its results to ofmaps once (O_2). Here, the first and the second read of ifmaps are for computing the mean (μ) and variance (σ^2) of pixels through an entire mini-batch per channel, whereas the last read is for normalization. These multiple ifmap reads are due to the dependency between the computational nodes within a BN layer (i.e., computing variance needs mean, and normalization needs mean and variance). Similarly, on the backward pass, data dependency exists but in a reverse direction. The partial derivatives on the ofmap from the ReLU layer are read multiple times to compute the partial derivatives on γ and β, which are needed for the partial derivatives on the ifmap.

We separate the normalization operations from mean and variance computation in a BN layer, calling the divided layers as sub-BN1 and sub-BN2, as depicted in the lower half of Figure 5(a). Fission enables both sub-BNx layers to be fused with its adjacent layers; sub-BN1 glues to CONV1 (the CONV layer that precedes the BN layer being split) whereas sub-BN2 glues to ReLU and CONV2 (the CONV layer that follows the BN layer in Figure 5). Fission provides an opportunity to handle operations of each sub-BNx during reading and writing ifmaps/ofmaps in BN's preceding and following CONV layers without additional off-chip memory access. Without Fission, a BN layer can be fused with either CONV1 or ReLU-CONV2 only, which prevents the maximum reduction of memory accesses by Fusion.

For the two aforementioned dependencies within a BN layer (computing variance needs mean, and normalization needs mean and variance), Fission copes with the latter, but the former still exists, especially on the forward pass. We eliminate this dependency by exploiting a simple mathematical formula below:

$$V(X) = E((X - E(X))^2) = E(X^2) - E(X)^2$$

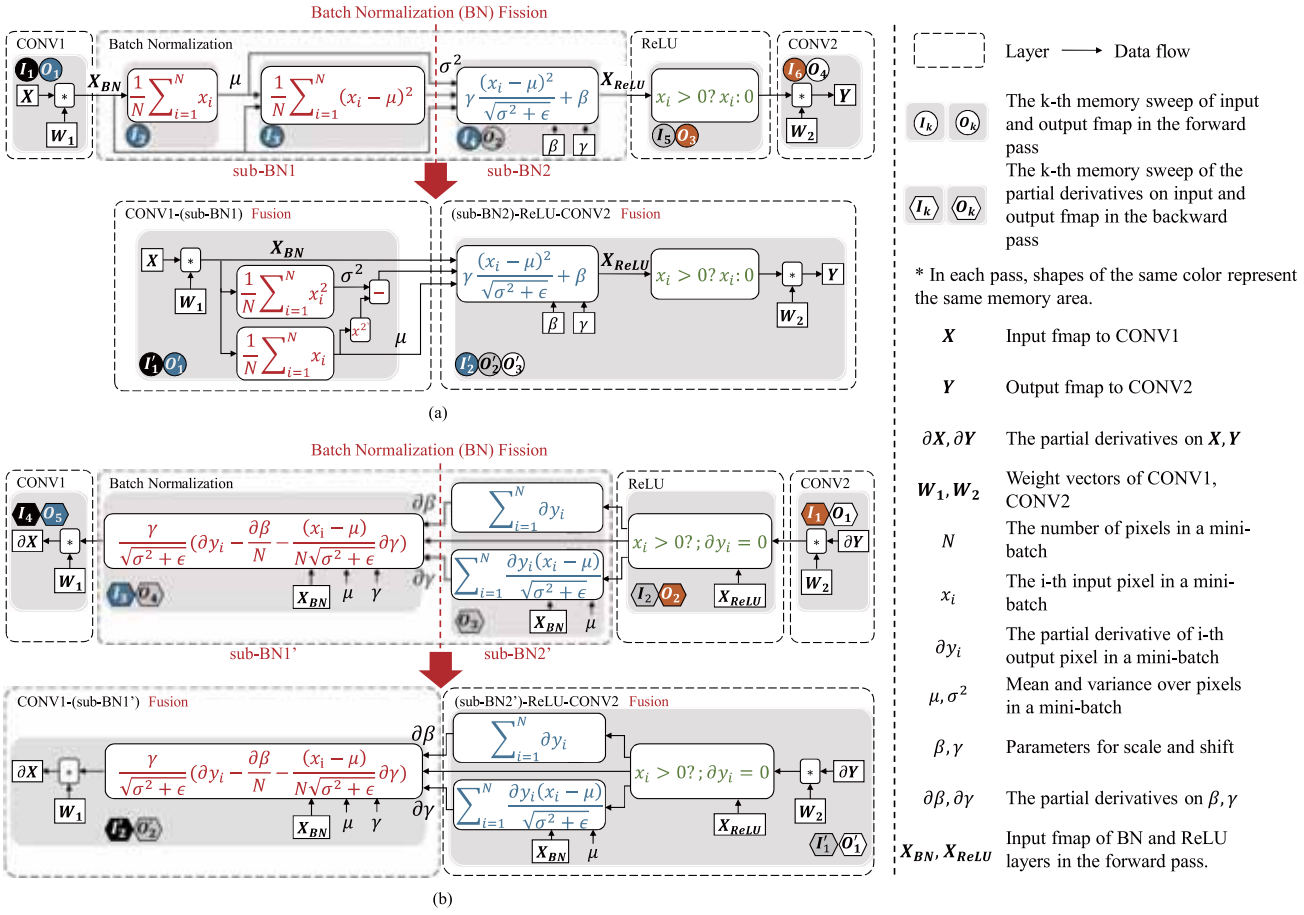

Figure 5. Illustration of BN Fission-n-Fusion on (a) the forward pass and (b) the backward pass. We present data dependency with arrows, memory sweeps (either reading or writing 100+ feature maps across an entire mini-batch per channel) as grey boxes, and multiple memory accesses to the same feature map with shapes of the same color. A BN layer is first divided into two sub-layers and then fused with the preceding CONV and the following CONV (+ReLU) layers, respectively.

That is, we can compute the per-channel variance of the pixels across a mini-batch of BN's ifmaps by computing $E(X^2)$ together with $E(X)$ from a single memory sweep. This mean/variance fusion (MVF) enables the two memory sweeps (I_2, I_3) within sub-BN1 to be merged with O_1 in CONV1 through Fusion. Computing the expectation of the square ($E(X^2)$) is more susceptible to accuracy errors which are inherent in floating-point arithmetic compared to computing $E(X)$. If it affects the accuracy of the network, we can use higher-precision representations (e.g., double-precision) to store intermediate data. Because BN is limited by main-memory bandwidth even after applying BNFF, using higher-precision representations and arithmetic does not impact training performance. During experiments, we observed that using single-precision floating-point arithmetic is good enough for calculating $E(X^2)$.

To fuse the first sub-BN1 layer with the CONV1 layer, we simultaneously perform both operations: convolution of CONV1 and accumulating x_i and ${x_i}^2$ from all pixels of CONV1's ofmaps over a mini-batch of BN on each channel. This ends up making one fused layer, CONV1-(sub-BN1), removing all memory accesses of sub-BN1. The second sub-BN2 layer is fused with both the ReLU layer and the CONV2 layer; the fused (sub-BN2)-ReLU-CONV2 layer perform normalization, ReLU, and convolution all together.

Because ReLU performs element-wise clipping, the recent CNN library we use (Intel, 2016) fuses a ReLU layer to its preceding CONV layer in the process of creating the ofmaps of the CONV layer. However, the latest CNN models might put ReLU layers in a different order. For example, in DenseNet, a ReLU layer is placed prior to the following CONV layer, and hence the aforementioned fusion implementation does not work. Our ReLU-CONV fusion (RCF) implementation executes the ReLU operation in the process of reading the ifmaps of the following CONV layer, removing memory access by the ReLU layer. Putting all the proposed solutions together, three memory sweeps (O_1, I_2, I_3) are reduced into one sweep (O_1') at the first fused layer,

and five (I_4, I_5, I_6, O_2, O_3) into two (I_2', O_2') at the second fused layer. A memory sweep (O_2') is required as it is used once again during the BN operation in the backward pass.

In the backward pass (backpropagation), BN first calculates the partial derivatives on γ and β, and then computes the partial derivatives on the ifmaps with them. This forms a strict data dependency. We separate operations that compute the partial derivatives on BN's ifmaps from calculating the partial derivatives on γ and β, calling the divided layers as sub-BN1' and sub-BN2', as depicted in Figure 5(b). Then, we combine the sub-BN1' layer with the preceding CONV1 and combine the sub-BN2' layer with both the ReLU layer and the following CONV2 layer. As opposed to the forward pass, the backward pass operations use not only the partial derivatives on ifmaps/ofmaps but also the ifmaps generated from the forward pass. Also, during the backward pass, CONV layers require twice as many computations and memory accesses as those of the forward pass to compute the partial derivatives on weight filters. This increases memory accesses that cannot be reduced by the proposed BNFF, making it less effective on the backward pass; but BNFF still removes five memory sweeps per BN layer.

BNFF can also be implemented across CPLs. This Inter-Composite-Layer Fusion (ICF) requires fusing the first sub-BN1 layer of a CPL after Fission with the corresponding Concat (or Split) layer, not the CONV layer. On the forward pass, because a Split layer is implemented as a pointer passing in our reference implementation, a sub-BN1 layer is fused with a Concat layer. On the backward pass, the sub-BN1' layer is fused with the corresponding Split layer. This completely removes all memory accesses on BN layers within DenseNet's CPLs. We implemented BNFF within CPLs and present experimental results measured from the latest chip processor in Section 5. We estimate additional performance enhancement enabled by ICF, leaving implementation for future work.

4 Experimental Setup

We quantify the performance improvement of the proposed BN Fission-n-Fusion using DenseNet-121, whose accuracy is on a par with ResNet-50 at a lower computation cost. DenseNet-121 was trained with Imagenet dataset (Russakovsky et al., 2015) and the mini-batch size was set to 120. We used Caffe (Jia et al., 2014) (Intel Caffe 1.0.7, which was released December 2017 (Intel, 2017)) as a reference CNN framework.

We used Intel's latest chip multiprocessor (Skylake-based Xeon Gold 6138 (Doweck et al., 2017)) for performance evaluation by default. The system consists of 20 cores with 40 AVX-512 FMA (fused multiply-add) units per socket, achieving a peak performance of 3.34TFLOPS with two sockets. Two sockets have twelve memory channels, each with DDR4-2400 DRAM modules achieving up to 230.4GB/s. To observe performance trends with a higher FLOP/B ratio, we also controlled the data transfer rates of the memory channels.

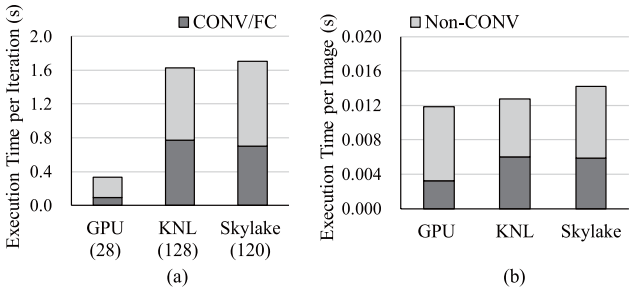

Figure 6. CONV/FC vs. non-CONV execution time of DenseNet-121 among data-parallel architectures: GPU, KNL (Knights Landing), and Skylake-based Xeon. (a) Execution time per iteration (the numbers in parentheses indicate mini-batch size), (b) Execution time per image (normalized by the mini-batch size.)

Table 1. Peak single-precision floating point performance and peak memory bandwidth on the latest data-parallel architectures.

Architectures	TFLOPS	Main-memory BW (GB/s)
Intel Xeon Skylake (2-socket)	3.34	230.4
Intel Xeon Phi Knights Landing	5.30	400.0
Nvidia GPU Pascal Titan X	10.0	480.0

We used Intel's Skylake-based Xeon processor because it supports a highly-optimized open-source CNN library (MKL-DNN v0.11 (Intel, 2016)) which can be modified for implementing BNFF. It supports extracting a variety of detailed hardware statistics, which can be helpful for analyzing BNFF benefits as well as for debugging. Figure 6 compares the execution time of DenseNet-121 over Pascal-based GPU (Titan X (Foley & Danskin, 2017)) using cuDNN, Knights Landing Xeon Phi (KNL) (Sodani et al., 2016), and Skylake-based Xeon. We set the mini-batch sizes of KNL and Skylake-based Xeon to 128 and 120, respectively. However, due to memory capacity limitation, we set the mini-batch size of the Pascal-based GPU to 28.

All three architectures spend more time on non-CONV layers compared to CONV layers, demonstrating the importance of optimizing these non-CONV layers (see Figure 6(a)). In Table 1, Skylake-based Xeon has 1.6× and 3.0× lower peak performance than KNL and GPU. However, execution time per image is similar to the others (see Figure 6(b)) because Skylake-based Xeon fully utilizes computing units on all CONV layers compared to the other architectures.

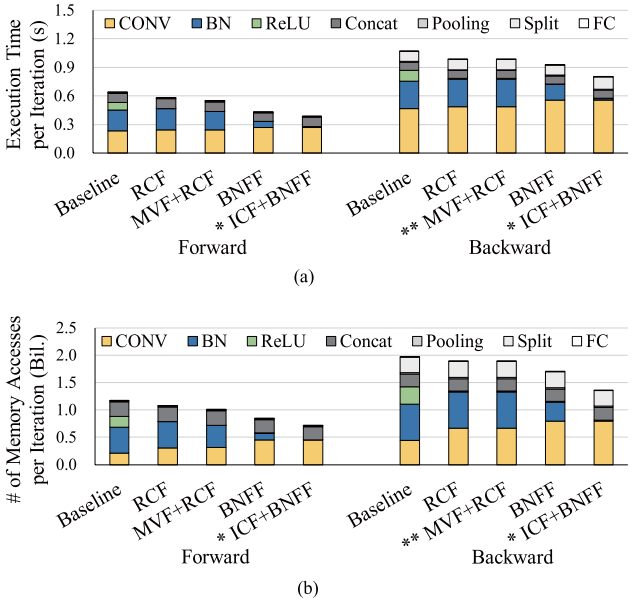

Figure 7. For DenseNet-121, (a) execution time and (b) the number of memory accesses per iteration by applying RCF (ReLU-CONV Fusion), RCF & MVF (Mean/Variance Fusion), BNFF (BN Fission-n-Fusion), and BNFF & ICF (Inter Composite-layer Fusion). Mini-batch size of 120 was used. *ICF improvement was estimated while the others are based on measurement from real machines. **MVF is not applicable to backward pass.

5 Evaluation

We provide the evaluation results of applying BN Fission-n-Fusion on DenseNet-121 training. To understand the quantitative improvements in detail, we have chosen four different scenarios and have evaluated their execution time and the number of memory accesses. The four scenarios are RCF (ReLU-CONV Fusion), MVF (Mean/Variance Fusion) together with RCF, BNFF (BN Fission-n-Fusion) that includes both MVF and RCF, and BNFF with ICF (Inter Composite-layer Fusion). While the performance improvement of RCF, MVF, and BNFF are from real-machine experiments, the improvement of ICF was estimated in line with BNFF improvement. The results are plotted in Figure 7. As a quick summary, the gain of BNFF over the baseline turns out to be 47.9% for the forward pass and 15.4% for the backward pass, and overall 25.7% for the training process.

In the following, we discuss the results of the four different scenarios. First, when only RCF is applied, the overall execution speed is increased by 9.2%. For the baseline, the number of memory accesses by ReLU layers takes up 16.8% of the total memory accesses. By merging the ReLU layer with CONV layer, the merged layer ends up with much less computation and memory access time compared to the total time needed for ReLU and CONV. The gain is similar for the forward pass and the backward pass (see Figure 7). Second, when MVF is applied on top of RCF, the overall execution speed is increased by an additional 1.7% compared to RCF. Because MVF can be applied only to the forward pass, the gain is entirely from 5.5% of improvement in the forward pass. Third, when BNFF is applied, where BNFF includes both MVF and RCF, the overall execution speed is improved by 25.7% compared to the baseline and 14.8% compared to the MVF+RCF. By applying BNFF, memory access is reduced by 19.1%. Besides the reduced main-memory accesses, fewer subroutine calls and lower cache miss rates due to an improved cache pollution environment by Fusion also contribute to the performance gains. Lastly, when ICF is applied on top of BNFF, the overall execution speed is estimated to be increased by 43.7% compared to the baseline. With ICF, all the BN layers in DenseNet-121, including the ones that are on the boundaries of composite layers, benefit from Fission-n-Fusion. Thus, an additional 18% of improvement over BNFF is expected with ICF.

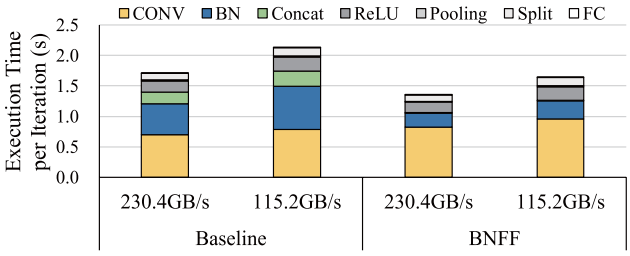

Figure 8. Execution time comparison of baseline and BNFF for 230.4GB/s and 115.2GB/s memory bandwidth.

BNFF divides a BN layer into sub-BN1 and sub-BN2 layers and then fuses them with the preceding and the following layers. Through this restructuring, the memory accesses of BN layers are entirely removed for the BN layers that do not cross the composite layer boundaries. As the result, the forward pass performance is improved by 47.9%. For the backward pass, however, the gain is only 15.4% because the CONV layers of backward pass need to perform twice as many computations and memory accesses compared to the forward pass. As CONV is heavier in computation for the backward pass, the relative portion of BN is smaller and the gain of BNFF is smaller, too. We also observed that a Split layer in the backward pass requires more frequent memory accesses compared to a Split layer in the forward pass. For the forward pass, only the pointer needs to be passed.

BNFF is more effective when the gap between computational power and main-memory bandwidth becomes wider (i.e., higher FLOP/B). As an additional evaluation, we tried reducing the peak memory bandwidth to the half (115.2GB/s) of the original, and the evaluation results are shown in Figure 8. For the baseline, the portion of non-CONV layers in the total execution time increases from 58.9% to 63.0% as the peak memory bandwidth is reduced by half. This is because the non-CONV layers are relatively

more sensitive to memory bandwidth, whereas the CONV layers are more compute-intensive. Therefore, it can be seen that optimizing memory access of non-CONV layers is important. For BNFF, both non-CONV and CONV layers suffer from the reduced memory bandwidth. Because many of the BN layers were optimized by BNFF already, it turns out that the degradation level is comparable for both CONV and non-CONV layers. A large portion of the CONV layers in DenseNet-121 also demand high main-memory bandwidth because they have smaller weight matrices (mostly 1×1 and 3×3) and hence their performance is also influenced by the reduced main-memory bandwidth. The gain of BNFF turns out to be 30.1% for 115.2GB/s of peak main-memory bandwidth (c.f. 25.7% for 230.4GB/s).

We also evaluated BNFF on the Caffe GPU implementation. We used Nvidia CUTLASS (Kerr et al., 2017), an open-source linear algebra library which enables us to implement BNFF, because other highly-optimized but closed-source GPU libraries such as cuBLAS (NVIDIA) and cuDNN (Chetlur et al., 2014) are difficult to modify.[3] Comparing the baseline with the CUTLASS library, we gained a 17.4% overall speedup by applying BNFF.

6 Related Work

There has been a large body of previous approaches to reduce memory accesses through increasing data reuse, both in on-chip and off-chip memory. We categorized the approaches into several groups, according to their purposes.

Maximizing data reuse: To reduce memory access cost, many proposed hardware accelerators have tried to maximize data reuse. DianNao (Chen et al., 2014a) optimized memory access to individual storage structures of weights, input feature maps, and output feature maps, thereby alleviating inefficiencies in accessing off-chip memory. DaDianNao (Chen et al., 2014b), following DianNao (Chen et al., 2014a), also lowered off-chip memory accesses by putting all the weights on the on-chip memory. With regard to the on-chip data transfer, a dataflow scheme called row stationary enables near-optimal data reuse for the CONV layers (Chen et al., 2016b). Most of these proposals are limited to the inference process.

Pruning and approximate computing: By eliminating redundant parameters in weights and feature maps, or reducing their precision, their data sizes could be greatly reduced, leading to reduction in memory accesses. Deep compression (Han et al., 2016b) reduces the model size of VGG-16 up to 49× by applying network pruning and quantization. EIE (Han et al., 2016a) compresses the weights and the input feature maps. It also addresses the irregular computation problem, a disadvantage coming from pruned sparse matrices. CirCNN (Ding et al., 2017) uses circulant matrices to reduce computation and time complexity, with a minor accuracy drop. The aforementioned approaches mostly focused on the CONV/FC layers.

Fusing and blending layers: Fused-layer (Alwani et al., 2016) is similar to our work as it fuses multiple CNN layers to exploit inter-layer data reusability; experiments on the VGGNet-E with FPGAs have shown a 95% memory transfer reduction per image. However, Fused-layer differs from our work in that we target BN and training process, where tight dependency over a large volume of data makes fusing multiple CONV layers a daunting task. Many machine learning frameworks, such as Caffe (Intel, 2017) and TensorFlow (Abadi et al., 2016), have already implemented fusing ReLU layers with the CONV layers. Similar to our approach, they also target to optimize inter-layer data reuse. However, there are limited potentials in the work because (1) they only combine CONV-ReLU layers, and (2) they do not concern BN layers; due to the complex data dependency, BN fusion is hardly available without fission as presented in this paper. To the best of our knowledge, none of the frameworks have tried fusing the BN layers with others.

Training acceleration: The optimization strategies above mainly target the inference process. Several studies accelerate the training process (De Sa et al., 2017; Ding et al., 2017; Rhu et al., 2016; Venkataramani et al., 2017), but none of those focused on the non-CONV layers, taking a significant portion of training time of the latest CNN models.

7 Conclusion

The existing studies on CNN acceleration were mainly limited to convolutional (CONV) and fully-connected (FC) layers. CNN models, however, are continuously evolving and the latest models can have hundreds of layers consisting of a variety of layer types. Among the non-CONV layers of the latest CNN models, we have found that batch normalization (BN) layers consume a significant portion of the execution time during training. A further analysis on BN's computation and memory access characteristics showed that the sequential and the less computationally-intensive nature of calculations with strict dependency over a large dataset causes an excessive memory access demand and makes fusing multiple CONV layers a daunting task. To address the issue, we have proposed a new type of CNN acceleration called Fission-n-Fusion, where BN is restructured to reduce memory access. Experiments on a latest chip multiprocessor showed that the proposed BN restructuring can improve the training performance of DenseNet-121 by 47.9% for forward pass and by 15.4% for backward pass, leading to overall 25.7% improvement. Applying the BN restructuring to GPU with an open-source linear algebra library also improves performance by 17.4%.

[3] Compared to the cuDNN implementation used in Section 4, the baseline CUTLASS implementation is 3.6× slower.

REFERENCES

Abadi, M., Barham, P., Chen, J., Chen, Z., Davis, A., Dean, J., Devin, M., Ghemawat, S., Irving, G., Isard, M., Kudlur, M., Levenberg, J., Monga, R., Moore, S., Murray, D. G., Steiner, B., Tucker, P., Vasudevan, V., Warden, P., Wicke, M., Yu, Y., and Zheng, X. Tensorflow: A system for large-scale machine learning. In *12th USENIX Symposium on Operating Systems Design and Implementation (OSDI)*, pp. 265–283, 2016.

Albericio, J., Judd, P., Hetherington, T., Aamodt, T., Jerger, N. E., and Moshovos, A. Cnvlutin: Ineffectual-Neuron-Free Deep Neural Network Computing. In *Proceedings of the 42nd Annual International Symposium on Computer Architecture (ISCA)*, 2016.

Alwani, M., Chen, H., Ferdman, M., and Milder, P. Fused-layer CNN accelerators. In *Proceedings of the 49th Annual IEEE/ACM International Symposium on Microarchitecture (MICRO)*, 2016.

Bergstra, J. and Bengio, Y. Random search for hyper-parameter optimization. *Journal of Machine Learning Research*, 13(Feb):281–305, 2012.

Canziani, A., Paszke, A., and Culurciello, E. An Analysis of Deep Neural Network Models for Practical Applications. *ArXiv e-prints*, May 2016.

Chen, T., Du, Z., Sun, N., Wang, J., Wu, C., Chen, Y., and Temam, O. DianNao: A Small-Footprint High-Throughput Accelerator for Ubiquitous Machine-Learning. In *Proceedings of the 19th International Conference on Architectural Support for Programming Languages and Operating Systems (ASPLOS)*, 2014a.

Chen, X., Duan, Y., Houthooft, R., Schulman, J., Sutskever, I., and Abbeel, P. Infogan: Interpretable representation learning by information maximizing generative adversarial nets. In *Advances in Neural Information Processing Systems*, pp. 2172–2180, 2016a.

Chen, Y., Luo, T., Liu, S., Zhang, S., He, L., Wang, J., Li, L., Chen, T., Xu, Z., Sun, N., and Temam, O. DaDianNao: A Machine-Learning Supercomputer. In *Proceedings of the 47th Annual IEEE/ACM International Symposium on Microarchitecture (MICRO)*, 2014b.

Chen, Y., Emer, J., and Sze, V. Eyeriss: A Spatial Architecture for Energy-Efficient Dataflow for Convolutional Neural Networks. In *Proceedings of the 42nd Annual International Symposium on Computer Architecture (ISCA)*, 2016b.

Chetlur, S., Woolley, C., Vandermersch, P., Cohen, J., Tran, J., Catanzaro, B., and Shelhamer, E. cuDNN: Efficient Primitives for Deep Learning. *ArXiv e-prints*, October 2014.

Chi, P., Li, S., Xu, C., Zhang, T., Zhao, J., Liu, Y., Wang, Y., and Xie, Y. PRIME: A Novel Processing-in-Memory Architecture for Neural Network Computation in ReRAM-Based Main Memory. In *Proceedings of the 42nd Annual International Symposium on Computer Architecture (ISCA)*, 2016.

Cogswell, M., Ahmed, F., Girshick, R., Zitnick, L., and Batra, D. Reducing overfitting in deep networks by decorrelating representations. *International Conference on Learning Representations*, 2016.

De Sa, C., Feldman, M., Ré, C., and Olukotun, K. Understanding and Optimizing Asynchronous Low-Precision Stochastic Gradient Descent. In *Proceedings of the 44th Annual International Symposium on Computer Architecture (ISCA)*, 2017.

Ding, C., Liao, S., Wang, Y., Li, Z., Liu, N., Zhuo, Y., Wang, C., Qian, X., Bai, Y., Yuan, G., Ma, X., Zhang, Y., Tang, J., Qiu, Q., Lin, X., and Yuan, B. CirCNN: Accelerating and Compressing Deep Neural Networks Using Block-circulant Weight Matrices. In *Proceedings of the 50th Annual IEEE/ACM International Symposium on Microarchitecture (MICRO)*, 2017.

Doweck, J., Kao, W. F., y. Lu, A. K., Mandelblat, J., Rahatekar, A., Rappoport, L., Rotem, E., Yasin, A., and Yoaz, A. Inside 6th-Generation Intel Core: New Microarchitecture Code-Named Skylake. *Micro, IEEE*, 37(2), Mar 2017.

Du, Z., Fasthuber, R., Chen, T., Ienne, P., Li, L., Luo, T., Feng, X., Chen, Y., and Temam, O. ShiDianNao: Shifting vision processing closer to the sensor. In *Proceedings of the 42nd Annual International Symposium on Computer Architecture (ISCA)*, 2015.

Foley, D. and Danskin, J. Ultra-Performance Pascal GPU and NVLink Interconnect. *Micro, IEEE*, 37(2), Mar/Apr 2017.

Goyal, P., Dollár, P., Girshick, R. B., Noordhuis, P., Wesolowski, L., Kyrola, A., Tulloch, A., Jia, Y., and He, K. Accurate, Large Minibatch SGD: Training ImageNet in 1 Hour. *ArXiv e-prints*, June 2017.

Han, S., Pool, J., Tran, J., and Dally, W. J. Learning both weights and connections for efficient neural network. In *Proceedings of the 28th International Conference on Neural Information Processing Systems (NIPS)*, 2015.

Han, S., Liu, X., Mao, H., Pu, J., Pedram, A., Horowitz, M. A., and Dally, W. J. EIE: efficient inference engine on compressed deep neural network. In *Proceedings of the 42nd Annual International Symposium on Computer Architecture (ISCA)*, 2016a.

Han, S., Mao, H., and Dally, W. J. Deep Compression: Compressing Deep Neural Networks with Pruning, Trained Quantization and Huffman Coding. In *International Conference on Learning Representations (ICLR)*, 2016b.

He, K., Zhang, X., Ren, S., and Sun, J. Identity Mappings in Deep Residual Networks. *ArXiv e-prints*, March 2016a.

He, K., Zhang, X., Ren, S., and Sun, J. Deep Residual Learning for Image Recognition. In *Proceedings of the IEEE Conference on Computer Vision and Pattern Recognition (CVPR)*, 2016b.

Howard, A. G., Zhu, M., Chen, B., Kalenichenko, D., Wang, W., Weyand, T., Andreetto, M., and Adam, H. Mobilenets: Efficient convolutional neural networks for mobile vision applications. *ArXiv e-prints*, April 2017.

Huang, G., Liu, Z., van der Maaten, L., and Weinberger, K. Q. Densely connected convolutional networks. In *Proceedings of the IEEE Conference on Computer Vision and Pattern Recognition (CVPR)*, 2017.

Intel. Intel(R) Math Kernel Library for Deep Neural Networks, 2016. URL https://github.com/01org/mkl-dnn.

Intel. Intel(R) Distribution of Caffe, December 2017. URL https://github.com/intel/caffe.

Ioffe, S. and Szegedy, C. Batch Normalization: Accelerating Deep Network Training by Reducing Internal Covariate Shift. In *Proceedings of the 32nd International Conference on Machine Learning (ICML)*, 2015.

Jia, Y., Shelhamer, E., Donahue, J., Karayev, S., Long, J., Girshick, R. B., Guadarrama, S., and Darrell, T. Caffe: Convolutional Architecture for Fast Feature Embedding. *ArXiv e-prints*, June 2014.

Jouppi, N. P., Young, C., Patil, N., Patterson, D., Agrawal, G., Bajwa, R., Bates, S., Bhatia, S., Boden, N., Borchers, A., Boyle, R., Cantin, P.-l., Chao, C., Clark, C., Coriell, J., Daley, M., Dau, M., Dean, J., Gelb, B., Ghaemmaghami, T. V., Gottipati, R., Gulland, W., Hagmann, R., Ho, C. R., Hogberg, D., Hu, J., Hundt, R., Hurt, D., Ibarz, J., Jaffey, A., Jaworski, A., Kaplan, A., Khaitan, H., Killebrew, D., Koch, A., Kumar, N., Lacy, S., Laudon, J., Law, J., Le, D., Leary, C., Liu, Z., Lucke, K., Lundin, A., MacKean, G., Maggiore, A., Mahony, M., Miller, K., Nagarajan, R., Narayanaswami, R., Ni, R., Nix, K., Norrie, T., Omernick, M., Penukonda, N., Phelps, A., Ross, J., Ross, M., Salek, A., Samadiani, E., Severn, C., Sizikov, G., Snelham, M., Souter, J., Steinberg, D., Swing, A., Tan, M., Thorson, G., Tian, B., Toma, H., Tuttle, E., Vasudevan, V., Walter, R., Wang, W., Wilcox, E., and Yoon, D. H. In-datacenter Performance Analysis of a Tensor Processing Unit. In *Proceedings of the 44th Annual International Symposium on Computer Architecture (ISCA)*, 2017.

Kerr, A., Merrill, D., Demouth, J., and Tran, J. CUTLASS: Fast Linear Algebra in CUDA C++, December 2017. URL https://devblogs.nvidia.com/cutlass-linear-algebra-cuda.

Kim, D., Kung, J., Chai, S., Yalamanchili, S., and Mukhopadhyay, S. Neurocube: A Programmable Digital Neuromorphic Architecture with High-Density 3D Memory. In *Proceedings of the 42nd Annual International Symposium on Computer Architecture (ISCA)*, 2016.

Krizhevsky, A., Sutskever, I., and Hinton, G. E. ImageNet Classification with Deep Convolutional Neural Networks. In *Proceedings of the 25th International Conference on Neural Information Processing Systems (NIPS)*, 2012.

NVIDIA. NVIDIA cuBLAS Library. URL https://developer.nvidia.com/cublas.

Rhu, M., Gimelshein, N., Clemons, J., Zulfiqar, A., and W. Keckler, S. vDNN: Virtualized deep neural networks for scalable, memory-efficient neural network design. In *Proceedings of the 49th Annual IEEE/ACM International Symposium on Microarchitecture (MICRO)*, 2016.

Russakovsky, O., Deng, J., Su, H., Krause, J., Satheesh, S., Ma, S., Huang, Z., Karpathy, A., Khosla, A., Bernstein, M., Berg, A. C., and Fei-Fei, L. ImageNet Large Scale Visual Recognition Challenge. *International Journal of Computer Vision (IJCV)*, 115(3):211–252, 2015. doi: 10.1007/s11263-015-0816-y.

Shafiee, A., Nag, A., Muralimanohar, N., and Balasubramonian, R. ISAAC: A Convolutional Neural Network Accelerator with In-Situ Analog Arithmetic in Crossbars. In *Proceedings of the 42nd Annual International Symposium on Computer Architecture (ISCA)*, 2016.

Silver, D., Huang, A., Maddison, C., Guez, A., Sifre, L., van den Driessche, G., Schrittwieser, J., Antonoglou, I., Panneershelvam, V., Lanctot, M., Dieleman, S., Grewe, D., Nham, J., Kalchbrenner, N., Sutskever, I., Lillicrap, T., Leach, M., Kavukcuoglu, K., Graepel, T., and Hassabis, D. Mastering the game of Go with deep neural networks and tree search. *Nature*, 529:484–489, 01 2016.

Simonyan, K. and Zisserman, A. Very Deep Convolutional Networks for Large-Scale Image Recognition. *ArXiv e-prints*, September 2014.

Snoek, J., Larochelle, H., and Adams, R. P. Practical bayesian optimization of machine learning algorithms. In *Advances in neural information processing systems*, pp. 2951–2959, 2012.

Sodani, A., Gramunt, R., Corbal, J., Kim, H.-S., Vinod, K., Chinthamani, S., Hutsell, S., Agarwal, R., and Liu, Y.-C. Knights Landing: Second Generation Intel Xeon Phi Product. *Micro, IEEE*, 36(2), Mar/Apr 2016.

Sriniva, S. and Babu, R. V. Data-free parameter pruning for Deep Neural Networks. *ArXiv e-prints*, July 2015.

Srivastava, N., Hinton, G., Krizhevsky, A., Sutskever, I., and Salakhutdinov, R. Dropout: a simple way to prevent neural networks from overfitting. *Journal of Machine Learning Research (JMLR)*, 15, 2014.

Szegedy, C., Ioffe, S., Vanhoucke, V., and Alemi, A. Inception-v4, Inception-ResNet and the Impact of Residual Connections on Learning. *ArXiv e-prints*, February 2016.

Venkataramani, S., Ranjan, A., Banerjee, S., Das, D., Avancha, S., Jagannathan, A., Durg, A., Nagaraj, D., Kaul, B., Dubey, P., and Raghunathan, A. ScaleDeep: A Scalable Compute Architecture for Learning and Evaluating Deep Networks. In *Proceedings of the 44th Annual International Symposium on Computer Architecture (ISCA)*, 2017.

Xie, S., Girshick, R. B., Dollár, P., Tu, Z., and He, K. Aggregated Residual Transformations for Deep Neural Networks. *ArXiv e-prints*, November 2016.

Yang, S. densenet-github, 2017. URL https://github.com/shicai/DenseNet-Caffe.

Yang, X., Pu, J., Rister, B. B., Bhagdikar, N., Richardson, S., Kvatinsky, S., Ragan-Kelley, J., Pedram, A., and Horowitz, M. A Systematic Approach to Blocking Convolutional Neural Networks. *ArXiv e-prints*, June 2016.

Zhang, S., Du, Z., Zhang, L., Lan, H., Liu, S., Li, L., Guo, Q., Chen, T., and Chen, Y. Cambricon-X: An accelerator for sparse neural networks. In *Proceedings of the 49th Annual IEEE/ACM International Symposium on Microarchitecture (MICRO)*, 2016.